Development of a Control Platform for an Hybrid Dropfoot Orthosis

André Monteiro Santos Brás Couceiro
andre.couceiro@tecnico.ulisboa.pt

Instituto Superior Técnico, Universidade de Lisboa, Lisboa, Portugal

October 2017

Abstract

Within the scope of human gait aid systems, a control board capable of driving a Dropfoot orthotic device is proposed. The device acquires the required signals from four inertial units and six insole pressure sensors at a maximum selectable rate of 300 Hz, and controls a Functional Electro-Stimulation module as well as four channels of any kind of PWM controlled actuator (magneto-rheological dampers for example). Having wearability in mind, the board's final design should present an area of approximately half a credit card, and height not greater that 10 mm, given it was based in the design of a FlexSea Manage board. Algorithms may be generated from Simulink models in order to simplify the process, and data may be logged into an on-board memory or via micro USB port to a laptop. The board capability as a gait analyzing device was assessed by testing it for several trials, and the output capability was tested by direct commanding of the driving signal. The processing power outperforms other systems present in literature due to the advanced floating point processing unit included in the chosen 180MHz clock micro-controller. The main goal of this control board is not only to present itself as a solution for hybrid Dropfoot assistance orthoses, but to provide a truly wearable platform for research projects in the field of Rehabilitation Biomechanics.

Keywords: Ankle Biomechanics, Active Ankle-Foot Orthosis, FlexSea, Functional Electrostimulation, Prototyping Control Platform

1. Introduction

Dropfoot is a neuromuscular disturbance resulting in weakness of the ankle dorsiflexor muscles, most regularly "caused by stroke, cerebral palsy, multiple sclerosis and neurological trauma" [3]. Gait cycle abnormality regarding dropfoot usually consists in lifting the lower limb above regular gait needs in order to avoid toe drag (and subsequent stumbling), which translates into visibly increased knee flexion during swing. Current options to overcome such disabilities are the use of Ankle Foot Orthoses (AFOs), Functional Electrostimulation (FES) and surgical intervention[9].

Actuated types of AFO, defined as Active Ankle Foot Orthosis (AAFO) have also been proposed throughout the years, but commonly present an excessively large form factor due to the addition of the actuator, making it difficult to have them deployed under the concept of everyday use orthoses. Furthermore, the required computational power usually demanded addition of heavy control equipment in the past, impairing the portability of the system, however since then many technological advancements such as the advent of micro-controllers and embedded computers have been facilitating the prototyping and testing of new active devices. In order to develop an AAFO with increased levels of portability for the correction of the Dropfoot disability, a Magneto-Rheological Orthosis (MR Orthosis) was proposed in [11]. This design relies in the fact that the major actuation required for dropfoot correction is applying negative work to the ankle joint. For negative work, an active actuator (such as a DC motor) should not be necessary, so it is replaced by a MR damper and a spring system. Hybrid systems integrating AFO/AAFOs and FES were also proposed showing promising results, namely regarding muscle fatigue reduction.

This project presents a step towards the achievement of an MR Orthosis device, by proposing an electronic platform based on the FlexSea Manage [12] and capable of handling the sensor acquisition and processing, implementing the control methodology and driving the control actions to the MR

Dampers but also integrating the possibility of FES actuation.

2. Background

2.1. Human Gait Cycle

Human gait is a complex repetitive motion, consisting in the coordinated movement of the limbs and resulting in the body's locomotion [21]. The gait cycle is defined as "the time interval between two successive occurrences of one of the repetitive events of locomotion" [22]. Figure 1 presents the typical walking gait cycle division [25].

The cycle is divided into the stance and swing periods, which further divide into, respectively, five and three different phases. Stance starts when the *Initial Contact* of the foot with the ground (also known as *Heel Strike*) occurs, followed by *Loading Response* phase when body weight is shifted to the landing foot. Next, during *Mid Stance*, the opposite limb is elevated in the direction of locomotion (opposite limb Swing), making the body center of gravity move over the foot, which is followed by *Terminal Stance* when body weight is moved from the hind and midfoot to the forefoot, and opposite *Initial Contact* (*Heel Strike*) occurs. In *Pre Swing*, the elevation of the limb is prepared by gradually changing weight to the opposite leg. This phase ends when all weight has been transferred and the foot is just about to leave the ground by lifting the toe. This event is usually referred to as *Toe Off*, and marks the beginning of the Swing period. *Initial Swing* is the phase between *Toe Off* and the moment the knee is in maximum flexion and is followed by *Mid Swing* which ends when the tibia is vertically aligned. *Terminal Swing* ends when *Heel Strike* repeats, thus beginning a new cycle [25, 28, 16].

The ankle and foot play an important role in "progression and shock absorption during stance" [11, 34] and in creating pivotal systems (rockers) that preserve the momentum by letting the knee joint maintaining an extended position while the body moves [25].

Muscle activity during each phase is also represented in figure 1. At *Initial Contact*, the body continuously moves forward, rapidly loading the limb at the ankle joint, causing an external plantarflexion moment. This moment is counter-balanced by the internal moment generated mainly the *tibialis anterior* controlling the heel support period, the advance of the *tibia* and the forward body weight rolling on the heel [17]. This mechanism is also known as Controlled Plantarflexion.

During *Mid Stance*, the *triceps surae* group (*gastrocnemius* and *soleus* muscles) must resist the an external dorsiflexion moment caused by body advancement, controlling the motion of the tibia.

In *Terminal Stance*, the maximum dorsiflexion angle is reached [25].

Pre Swing is characterized by Power Plantarflexion that leads to an accelerated advancement of the limb. Such movement is provided by the contraction of the *triceps surae* muscles[16]. There is a peak plantarflexion angle at the moment of *Toe Off*.

During the Swing phase, the *triceps surae* and *tibialis anterior* control the foot to its neutral position. In *Initial* and *Mid Swing*, and in *Terminal Swing* the *tibialis anterior* and other dorsiflexor muscles strengthen their activity in order to ensure a neutral position for *Heel Strike* as well as to anticipate the heavy contraction required in the *Loading Response* phase [34, 17].

Figure 2 shows the normal evolution of the ankle angle throughout the gait cycle. Plantarflexion is considered negative and dorsiflexion positive in relation to the neutral position, foot perpendicular to the lower leg.

2.2. Dropfoot Gait Abnormality

The main symptoms that arise from the dropfoot disability are known as *foot-slap* and *toe-drag*, and are presented in figure 3. These are mainly caused by disruption of the motor control pathway of the anterior and lateral compartment muscles of the leg, namely the *tibialis anterior* [25, 15].

Foot-slap occurs after the *Initial Contact* or *Heel Strike* event. Instead of a controlled landing motion as in healthy *Loading Response* phase, the foot slaps the ground. *Inversion* and *Eversion* movements are also affected, so lateral ankle stability is reduced.

Toe-drag in the ground happens during Swing because of the poorly achieved toe clearance [25].

Patients will usually adopt compensatory strategies to overcome the dropfoot symptoms that change the way they walk, possibly developing further problems in other muscles and structures [28].

Ankle Foot Orthoses present themselves as the usual care solution for ankle-foot related disability correction [30]. The main goal of this mechanical devices is to improve the gait of affected individuals by controlling the joint motion, as they typically "support and align the ankle and the foot, suppress spastic and overpowering ankle and foot muscles, assist weak and paralyzed muscles of the joint, prevent or correct deformities and improve the functions of the ankle-foot complex" [11]. In the case of dropfoot patients, the action of an AFO should provide mediolateral stability of the ankle during the stance phase of gait and improve the swing phase of the disturbed leg while allowing free ankle plantarflexion and dorsiflexion during the stance phase since the plantarflexor muscles are frequently not affected [7]. According to the principle of operation, AFOs may be classified into three groups: Passive Rigid, Passive Dynamic or Active orthoses [13].

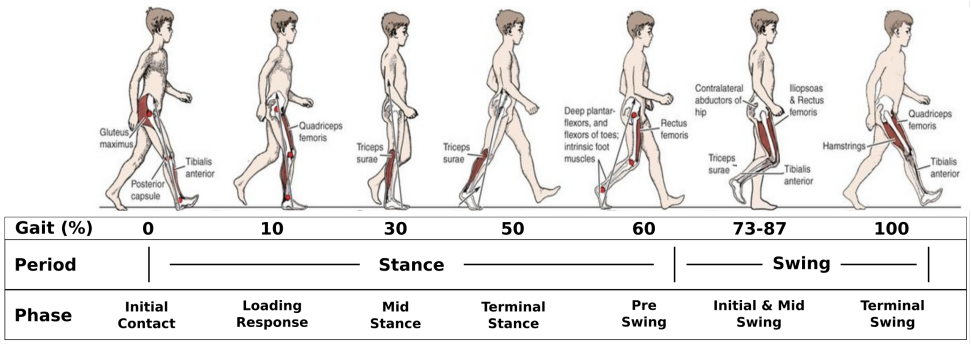

Figure 1: Walking Gait Cycle Representation.

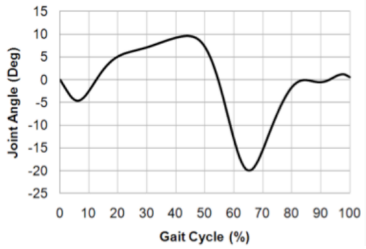

Figure 2: Ankle angle evolution over one walking gait cycle [35].

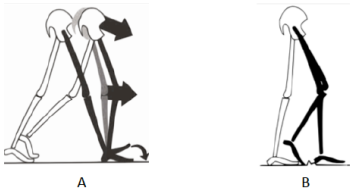

Figure 3: *Foot-slap* (A) and *toe-drag* (B) events in dropfoot patients.

The traditional Passive Rigid type consist in solid plastic braces, although they also may be manufactured from metal or composite materials, with any number of modifications, including articulated or hinged ankle joint [19].

Passive dynamic orthoses are AFO designs rely on characteristics such as material properties, component thickness, shape, springs, and fluid pressure dynamics to establish bending or rotational stiffness characteristics and to regulate the storage and return of mechanical energy [13].

Active ankle foot orthoses (AAFO) are devices that use motors, pumps, and actuators to actively control the magnitude of joint assistance and level of mechanical energy transferred [13]. A few examples of devices resulting from scientific efforts are Blaya's Force-Controllable Ankle Foot Orthosis [3], Chin's Pneumatic Power Harvesting Ankle-foot Orthosis [7], Ferris' Powered Ankle-foot Orthosis using Proportional Myoelectric Control [14] or Park's Bio-inspired Active Soft Orthotic Device [24]. Devices based in Magneto-Rhelogical fluid were also proposed, such as the i-AFO by Kikushi et al. [18] and Svensson et al. [32] Ankle-Foot-Orthosis.

The current real alternative to passive AFOs is the use of Functional Electrostimulation (FES) systems, already spread over the market under various forms. FES relies on the fact the the dropfoot patient's nerves and muscles are often still capable of producing contraction if the correct electrical excitation is applied, given the major causes for dropfoot are neuro related and do not necessarily imply lack of muscle capability. Same way as AFOs, the main goal of FES is to provide toe clearance during Swing, minimize foot-slap after Heel Strike and, if necessary, assist plantarflexion. This is achieved by providing electrical stimulus to targeted nerves through the use of electrodes (superficial or implantable), most commonly to the peroneal nerve in order to induce dorsiflexion, but also to other muscle groups in order to further enhance the patient's gait.

Regarding the stimulation signal, a rectangular shape has been suggested as optimal, defined by three parameters: Pulse frequency, Pulse width and Amplitude as shown in figure 4, and should provide both positive and negative charge in order to keep the tissues' pH levels in balance preventing damage. Pulse frequency is related to the stimulus type and amount of force to be produced (usually kept in the range 20 - 40 Hz), while Pulse width ($<$250 μs) and Amplitude ($<$120 mA over 500ohm in surface electrodes and $<$3 mA in implanted electrodes) are co-responsible for generating the required amount of ionic flow to trigger action potentials [10].

The concept of Hybrid Orthosis featuring complementary FES and AFO systems has existed in literature at least since 1984 [1], and more recently AAFO have also been integrated along with FES units. Typically, the mechanical part (AFO/AAFO) of hybrid orthoses provides stability of the lower limb and FES activates the extensor muscles only in order to produce movement,

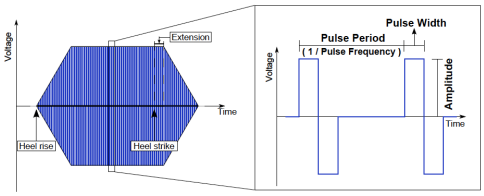

Figure 4: FES signal characteristics [10].

minimizing the negative effects of an exclusive FES system such as the rapid muscular fatigue and the lack of protection against falling either by destabilization or by electronics failure [26]. Examples of prototypes are Andrews et al. "Hybrid FES orthosis incorporating loop control and sensory feedback" [1], Phillips et al. "Electrical muscle stimulation in combination with a reciprocating gait orthosis for ambulation by paraplegics" [26], Popovic et al. "Hybrid Assistive System (HAS)" [27], who also documented an improvement in gait velocity and decrease in energy consumption, and Arnez-Paniagua et al. "A Hybrid Approach towards Assisting Ankle Joint of Paretic Patients" [2].

2.3. Control Board Introduction

As a start point for the development of the control board, a small review of the systems used in other AAFOs was performed and is presented in table 1. Commonly used sensors are Inertial Measuremnt Units for kinematics acquisition and pressure sensors for kinetics and event detection. It is also noticeable that most prototypes were not designed to be used in real world application due to lack of portability, with the exception of FES based devices. Even if exclusively considering systems that rely in embedded electronics, the number of control boards and or their dimensions is usually large enough that it adds to the overall system volume.

In reference [12], an embedded system for wearable robotics was developed, the FlexSEA. The main motivation of the project was to provide a general rapid prototyping platform, avoiding the need to re-design hard/software for each new research work in the field of wearable robotics. Following a business naming strategy, the system presents itself as a modular architecture, comprising three main levels/boards: *Plan*, *Manage* and *Execute* that communicate among each other. Figure 5 shows the original Manage and Execute boards. The Manage board was chosen as a base for the design for the control board because it holds the FlexSEA wide list of specifications:

- Reliability
- Processing Power (180MHz ARM Cortex-M4)
- Ease of Code Portability (C-Coded firmware)
- Maximum electronics embedded
- Fast Communication Peripherals (USB, I^2C, SPI, USART)
- Power Consumption
- Form Factor (40x40x10.7 mm)

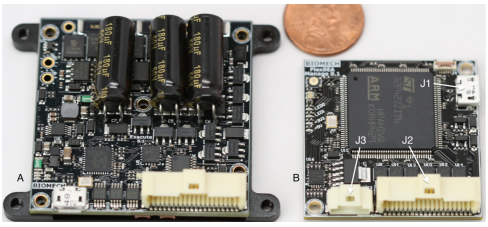

Figure 5: The FlexSEA boards: Execute (A) and Manage (B) [12].

In order to comply with the MR Orthosis needs and also to improve functions already present at the time, several Hard and Software developments were introduced.

The control board should be able to:

- Collect and filter data from the IMU group (4 channel I^2C)
- Collect and filter data from the FSR group (6 ADC)
- Compute the control actions (Processing Power)
- Drive the control signals to the MR Dampers, and/or (PWM MOSFET based driver)
- Communicate a control action to the FES module (UART + Protocol)

3. Implementation

The control board architecture is presented in figure 6, the main loop is clocked at 1 KHz. A brief explanation of the developed hardware and firmware strategies for handling the inputs and outputs is presented in this section.

3.0.1 Inertial Measurement Unit (IMU) Group

Acquisition of the four IMUs is possible by using an I^2C multiplexer for the *SDA* (data) line of the bus while all four IMU share the *SCLK* (clock) line.

The acquisition cycle for **each** IMU consists in the following chronological tasks:

- Reset FIFO
- Start FIFO operation (write Accelerometer and Gyroscope data at sample rate)
- Wait for a few packets to be written
- Stop FIFO operation
- Read first packet from FIFO
- Parse packet

Reference	Actuation	Sensors(Rate-Hz)		Control Board	Portability
		Kinematics	Kinetics	Processor/Interface(Clock-MHz)	
[4]	SEA (DC Motor+Spring)	Potentiometer(1000)	Capacitive Force Sensors(125)+Heel Switch(-)	CIO-DAS08/JR-AO+Linux	Fixed
[14]	DC Motor + Spring	-	EMG(1000)	dSPACE, Inc.+PC	Fixed
[18]	MR Rotary Brake	Potentiometer(125)	Foot Switches(125)	A/D,D/A module + PC	Fixed
[32]	MR Damper	Potentiometer(50)	-	PIC18F(40)	Fixed
[24]	Peumatic	Strain(50), 2xIMU(50)	FSR Insole(50)	Atmega328P(16),Atmega1280(16)	Fixed
[8]	FES	Goniometer(-)	Foot Switch Insole(-)	PIC18F4520(8)	High
[5]	FES	IMU(-)	FSR Insole(-)	ADuC831(16)	High
[29]	FES	-	Piezo-Resistive Insole(100)	AT89SS2(40)	High
[6]	FES	-	EMG(10K)	TMS320C32(¡60)+Host PC	High
[10]	FES	IMU(133)	FSR(133)	Atmega328P(16)	Possible
[2]	Hybrid	Motor Encoder(1000)	FSR(1000)	FPGA	Fixed

Table 1: Overview of control systems used in several FES and Orthotic research devices.

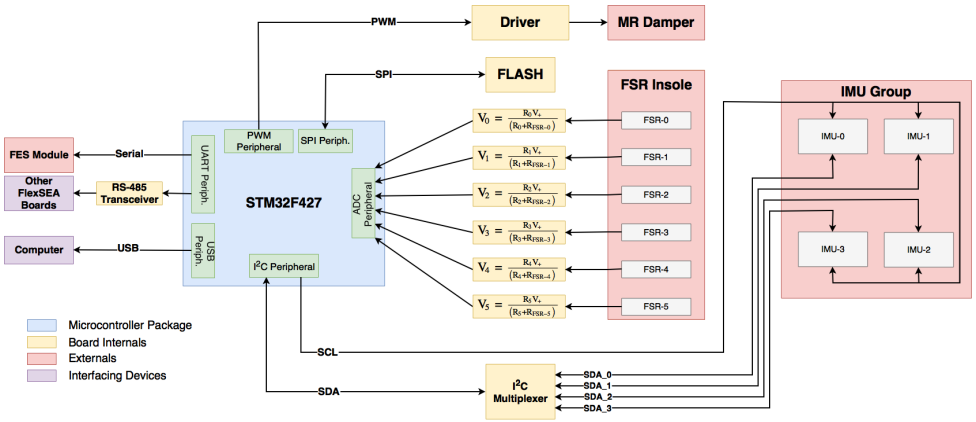

Figure 6: Control Board Architecture

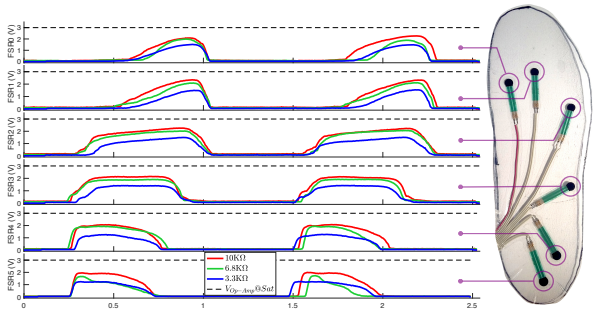

Figure 7: FSR Calibration Resistor Test

A State Machine combines the four multiplexed IMUs in order to get maximum synchronization (<300us between IMU_0 and IMU_3) and group sample rate (>300Hz).

3.0.2 Force Sensitive Resistor (FSR) Group

For the six FSR bundled in the FSR-Insole, a buffered voltage divider was designed and fed to the processor ADC inputs. The calibration resistor was selected so it would provide maximum signal resolution but prevent saturation at the input circuits (including the amplifier and the ADC pins). The value was 10 KΩ, and the saturation test run is presented in red (figure 7).

3.0.3 PWM Generation

The original Manage board does not make use the PWM module, consequentially a library was created in order to interact with the peripheral and enable four channels of PWM output. Figure 8 demonstrates generated 15 KHz PWM signals at channels 3 (25% duty cycle) and 4 (75% duty cycle).

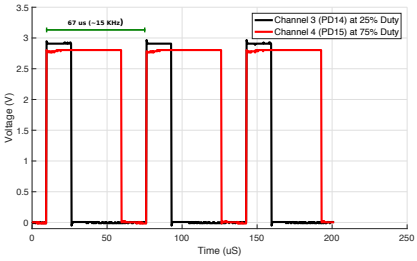

Figure 8: PWM signals at Channels 3 and 4 (15KHz).

3.0.4 FES Module Communication

The FES integration assumes the use of the module designed in [10], which complies with the following specifications:

- UART peripheral: USART-3

- Baud Rate: 111111 bits/s
- Data: [A,T,U,F] - 4 bytes
- Maximum Frequency: $\approx$ 200 Hz

Where A is the signal amplitude, T is the positive period, U is the negative period and F is the signal frequency. In order to communicate with the module, the protocol was implemented as in figure 9.

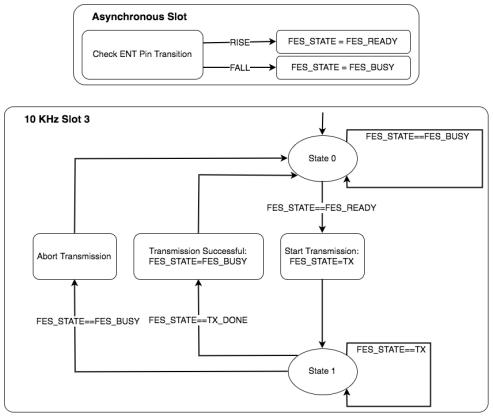

Figure 9: FES Module UART communication protocol

3.1. Development Tools

In order to test the presented concepts, a prototype that included all necessary circuits for signal acquisition and output was built based in the STM32F429I-DISC1 Development Kit by STMicroelectronics [31], which is fitted with the STM32F429ZI microcontroller. This microcontroller is full pin and code compatible with the STM32F427ZI fitted to the FlexSea Manage board. The final prototype is presented in figure 10, together with the IMU and FSR (insole) groups and the FES module.

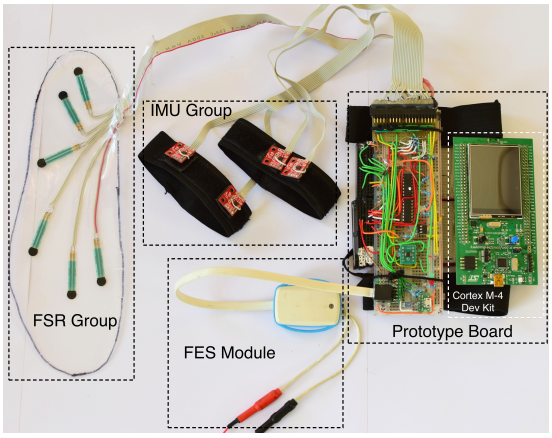

Figure 10: Board Prototype

The firmware is written in C, using the open source Eclipse environment for ARM development (GNU MCU Eclipse for ARM). Acknowledgment should be made that despite the fact that many features were introduced and removed, the code was written starting from the original Manage firmware by J. F. Duval and referenced in [12].

Accommodations were also made in order to allow future users to create their algorithms in higher level languages such as MATLAB/Simulink from MathWorks, Inc., and directly include the code as C source and header files into the Eclipse project.

4. Results

In order to test the viability of the prototype, several experiments were carried on a 25 year-old male, weight 75 Kg. Data was logged into the GUI via USB at 170 Hz (three data pages selected, auto mode) and processed using MATLAB. The trials included assessment of the ankle angle measurement accuracy from the IMU, regular gait analysis and bandwidth analysis by performing different gait speed exercises.

5. IMU

IMU calibration based in [33] was undertaken prior to all experiments in order to overcome the non accurate scaling, sensor axis misalignments, cross-axis sensitivities and non zero biases.

The filtering implementation applied to the IMU measurements for obtaining the IMU (and consequentially shin and foot) poses was derived from a zero-velocity aided inertial navigation system, as described in [20]. As largely suggested in literature, the ankle angle may be reduced to its saggital plane projection, which for the present frame, results from taking the difference between the pitch angle estimates from Shin and Foot. The pitch angles were computed for each IMU and averaged for the pair in order to get the Shin and Foot pitch.

Figure 11: IMU Positions

A first experiment was conducted in order to assess the validity of the IMU based estimated ankle

angles. A potentiometer was mounted in a goniometer, which was fitted in position for measuring the ankle angle. Simultaneously, the four IMU were placed as in figure 11. Both goniometer and IMU group were logged at a 170 Hz rate while the subject alternately dorsi and plantarflexed, starting from a neutral position (keeping the foot off the ground).

Figure 12 presents the comparison results between the goniometer and IMU measured signals. The Root Mean Square Error was 2.65 ° and the Correlation Coefficient was 98.78 %.

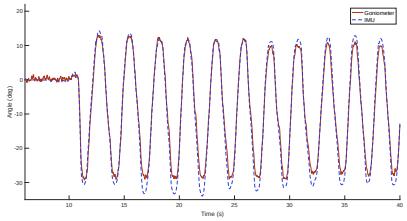

Figure 12: IMU vs Goniometer Ankle Angle

Pitch angles of the two pairs of IMU located at the leg and foot were computed from the accelerations and angular velocities. The results were averaged for each pair of IMU and are presented in figure 13. Given the frame represented in figure 11, the lower leg swings around a neutral angle of ≈ -100° and the foot around ≈ -35° (dotted green lines). The red dashed lines provide the Heel Strike instants.

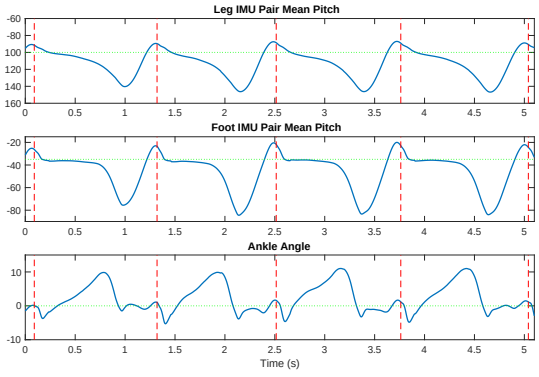

Figure 13: IMU Leg & Foot Pitch and Ankle Angle measurements: the red dashed lines mark the Heel Strike instants while the dotted green lines represent the neutral position angle reading for each variable with respect to the relevant frames.

As stated before, the ankle angle was calculated by subtracting the leg and foot pitch angles and removing the neutral angle in order to represent the final ankle angle relative to the lower limb neutral position (dotted green line). Dorsiflexion yields positive angles while plantarflexion yields negative

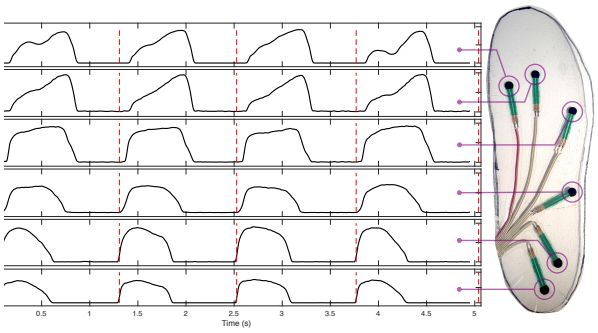

Figure 14: FSR Group Normalized Data: Normalized pressure data from the FSR insole. The red dashed lines mark the Heel Strike instants (at 5% threshold).

angles. The results are consistent to those reported in [10] and [11] in terms of gait timings, although the absolute angle values are smaller.

6. FSR

The FSR signal voltage was normalized within its scale (from 0-3.3V to 0-100%) and low-pass filtered at 20Hz. The resulting normalized pressures for a self-selected speed gait trial are presented in figure 14.

It is possible to observe the evolution of the pressure magnitude along the foot during each step out of four. From [23], the Center of Pressure (COP) was calculated as:

$$COP_x = \frac{\sum_{i=0}^{n-1} p_i x_i}{\sum_{i=0}^{n-1} p_i} \quad ; \quad COP_y = \frac{\sum_{i=0}^{n-1} p_i y_i}{\sum_{i=0}^{n-1} p_i} \tag{1}$$

where n represents the number of FSRs, p_i the pressure at FSR i and x_i and y_i respectively the coordinates of FSR i in the plane of the insole. The resulting evolution is presented in figure 15.

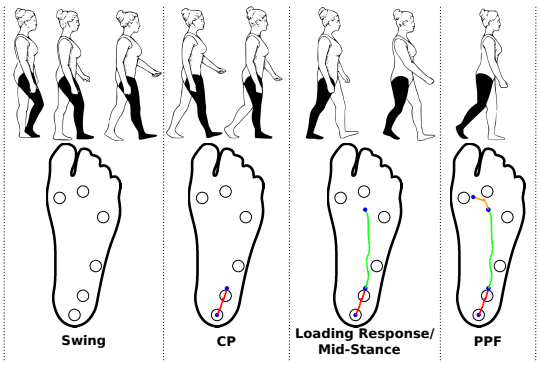

Figure 15: FSR based Center of Pressure evolution throughout the gait phases.

The combined results of the IMU and FSR group

sum (normalized and scaled representation) are shown in figure 16. By considering both the FSR contacts and the ankle angle at different time instants, it is possible to divide the step into four main phases: Controlled Plantarflexion (CP), Loading Response/Mid-Stance, Power Plantarflexion and Swing.

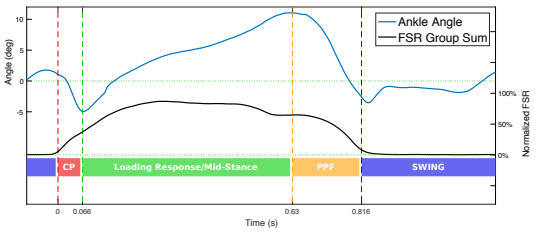

Figure 16: Gait Phase Detection

As stated before, Controlled Plantarflexion is the fastest event during regular gait, and also one of the most critical to take into account when correcting the Dropfoot disability, therefore an assessment of the capability of the system to acquire points during this phase was carried.

The CP phase for a fast gait trial logged at 167 Hz, 83 Hz and 42 Hz is illustrated in figure 17. At a logging frequency of 42 Hz it is not possible to fully characterize CP, which may jeopardize algorithms implementing IMU based phase detection or close loop control during this phase. In contrast, from a frequency of 83 Hz, CP is perfectly characterized, which proves the capability of the system. Up to 300 Hz log rate is possible with the control board.

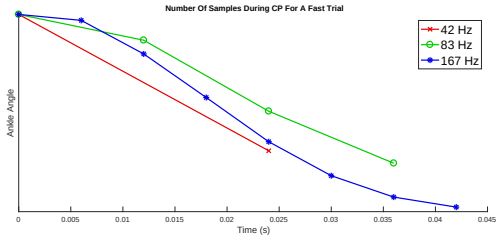

Figure 17: Ankle angle during CP at different log rates for a fast gait trial. At a frequency of 42 Hz there is no longer a smooth CP phase due to the reduced number of points.

7. Conclusions

From the acknowledgement of dropfoot related disabilities it is possible to idealize an efficient aiding device based in the concept of a magneto-rheological ankle foot orthosis complemented with passive mechanical elements. Furthermore, good results originating from the employment of functional electro-stimulation have been suggesting throughout the years that an hybrid orthotic device, combining both techniques, would potentially be able to achieve equivalent (or even improved) results while eliminating well known negative side-effects of the individual techniques, such as the increased power requirements of Active Ankle Foot Orthoses and the risk of muscle fatigue in the case of FES.

This work focused in the development of an electronic board capable of handling sensors, control algorithms and actuation of an hybrid orthosis. Starting from a review of control systems utilized in various research work, the most commonly used sensors for kinematic and kinetic characterization of the gait process (and/or other daily activities) were analyzed, namely the use of Inertial Measurement Units (four) and resistive insole pressure sensors (six). Regarding the actuation methods, magneto-rheological devices are usually PWM driven, and an external FES module was integrated via UART communication.

One of the most important concerns stated from the beginning was the board's form factor, which should be reduced enough in order to be almost transparent when compared to the remaining parts of the future system, but also the on-board processing power and ease of code development, so that increasingly complicated algorithms can not threaten the viability of the board. Having such specifications on the table, and in an effort not to incur in unnecessary "reinventing the wheel", an expression widely used by the FlexSea system creator, the FlexSea Manage board was introduced as a base design for the development of the board.

The IMU group acquisition at 300 Hz was successfully accomplished by using a multiplexing strategy, the insole FSR group acquisition was implemented and successfully calibrated as to avoid saturation, the FES module communication protocol was mirrored with a capability of 250 Hz parameter change rate and the PWM module was activated for four channels and encapsulated into a user friendly library in order to be readily available for future researchers. The logging capabilities of the original Manage board were improved due to the increased number of variables present in this project, and the Graphical User Interface core was also modified by adopting a multi-threaded software architecture. The embedded tools for C code generation from MATLAB were explored, enabling future users to develop high level algorithms inside Simulink which directly show in the board's firmware project. The final board dimensions should not greatly differ from the Manage (40x40x10.7 mm), thus complying with the reduced form factor requirement.

The main contribution of this work was to provide the control platform for a specific dropfoot correction device, but it ended up proposing a board potentially capable of being used in several investi-

gation prototypes (maybe even test products), presenting minor volume impact, increased computational capability and ease of code development.

References

[1] B. Andrews, R. Baxendale, R. Barnett, G. Phillips, T. Yamazaki, J. Paul, and P. Freeman. Hybrid fes orthosis incorporating closed loop control and sensory feedback. *Journal of biomedical engineering*, 10(2):189–195, 1988.

[2] V. Arnez-Paniagua, W. Huo, I. Colorado-Cervantes, S. Mohammed, and Y. Amirat. A hybrid approach towards assisting ankle joint of paretic patients. In *International Functional Electrical Stimulation Society conference (IFESS 2016)*, 2016.

[3] J. A. Blaya. *Force-controllable ankle foot orthosis (AFO) to assist drop foot gait*. PhD thesis, Massachusetts Institute of Technology, 2002.

[4] J. A. Blaya and H. Herr. Adaptive control of a variable-impedance ankle-foot orthosis to assist drop-foot gait. *IEEE Transactions on neural systems and rehabilitation engineering*, 12(1):24–31, 2004.

[5] P. P. Breen, G. J. Corley, D. T. O'Keeffe, R. Conway, and G. ÓLaighin. A programmable and portable nmes device for drop foot correction and blood flow assist applications. In *Engineering in Medicine and Biology Society, 2007. EMBS 2007. 29th Annual International Conference of the IEEE*, pages 2416–2419. IEEE, 2007.

[6] W.-L. Chen, S. Chen, C. Chen, C. Chou, Y. Shih, Y. Chen, and T. Kuo. Patient-driven loop control for ambulation function restoration in a non-invasive functional electrical stimulation system. *Disability and rehabilitation*, 32(1):65–71, 2010.

[7] R. Chin, E. T. Hsiao-Wecksler, E. Loth, G. Kogler, S. D. Manwaring, S. N. Tyson, K. A. Shorter, and J. N. Gilmer. A pneumatic power harvesting ankle-foot orthosis to prevent foot-drop. *Journal of neuroengineering and rehabilitation*, 6:19, June 2009.

[8] C. Chou, S. Chen, Y. Hwang, C. Ho, C. Chen, S. Chen, and Y. Chen. Application of fes for hemiplegia in extremity coordination training. In *Bioinformatics and Biomedical Engineering,(iCBBE) 2011 5th International Conference on*, pages 1–4. IEEE, 2011.

[9] K. Daniilidis, E. Jakubowitz, A. Thomann, S. Ettinger, C. Stukenborg-Colsman, and D. Yao. Does a foot-drop implant improve kinetic and kinematic parameters in the foot and ankle? *Archives of orthopaedic and trauma surgery*, 137:499–506, Apr. 2017.

[10] P. E. L. de Melo. *A Novel Functional Electrical Stimulation System and Strategies For Motor Rehabilitation*. phdthesis, Instituto Superio Tcnico, Universidade de Lisboa/Massachusetts Institute of Technology, 2014.

[11] A. R. C. Domingues. *On The Development Of An Active Softsecond-Skin Orthotic For Drop-foot Patients*. phdthesis, Instituto Superio Tcnico, Universidade de Lisboa/Massachusetts Institute of Technology, 2014.

[12] J.-F. Duval et al. Flexsea: flexible, scalable electronics architecture for wearable robotic applications. Master's thesis, Massachusetts Institute of Technology, 2015.

[13] M. C. Faustini, R. R. Neptune, R. H. Crawford, and S. J. Stanhope. Manufacture of passive dynamic ankle–foot orthoses using selective laser sintering. *IEEE transactions on biomedical engineering*, 55(2):784–790, 2008.

[14] D. P. Ferris, K. E. Gordon, G. S. Sawicki, and A. Peethambaran. An improved powered ankle-foot orthosis using proportional myoelectric control. *Gait & posture*, 23:425–428, June 2006.

[15] R. France. *Introduction to sports medicine and athletic training*. Nelson Education, 2010.

[16] V. H. Frankel and M. Nordin. Biomechanics of bone. *Basic biomechanics of the musculoskeletal system*, 3:26–59, 2001.

[17] J. R. Gage. An overview of normal walking. *Instructional course lectures*, 39:291–303, 1990.

[18] T. Kikuchi, S. Tanida, K. Otsuki, T. Kakehashi, and J. Furusho. Development of intelligent ankle-foot orthosis (i-afo) with mr fluid brake and control system for gait control. *Service Robotics and Mechatronics*, pages 75–80, 2010.

[19] P. M. Kluding, K. Dunning, M. W. ODell, S. S. Wu, J. Ginosian, J. Feld, and K. McBride. Foot drop stimulation versus ankle foot orthosis after stroke. *Stroke*, pages STROKEAHA–111, 2013.

[20] J.-O. Nilsson, I. Skog, P. Händel, and K. Hari. Foot-mounted ins for everybody-an open-source embedded implementation. In *Position Location and Navigation Symposium*

(PLANS), 2012 IEEE/ION, pages 140–145. Ieee, 2012.

[21] C. Norkin and P. Levangie. Joint structure & function: A comprehensive analysis (2nd). 448-493. *Ohio: Philadelphia. FA Davis Company*, 1992.

[22] T. F. Novacheck. The biomechanics of running. *Gait & posture*, 7(1):77–95, 1998.

[23] C. Park, S. Park, and C. H. Kim. Center of pressure of a human body using force sensing resistor. *Transactions of the Korean Institute of Electrical Engineers*, 63(12):1722–1725, 2014.

[24] Y. L. Park, B. r. Chen, D. Young, L. Stirling, R. J. Wood, E. Goldfield, and R. Nagpal. Bio-inspired active soft orthotic device for ankle foot pathologies. In *2011 IEEE/RSJ International Conference on Intelligent Robots and Systems*, pages 4488–4495, Sept 2011.

[25] J. Perry and J. Burnfield. Gait analysis: normal and pathological function. 1992. *Thorofare, NJ: Slack*, 1992.

[26] C. Phillips. Electrical muscle stimulation in combination with a reciprocating gait orthosis for ambulation by paraplegics. *Journal of biomedical engineering*, 11(4):338–344, 1989.

[27] D. Popovic, R. Tomovic, and L. Schwirtlich. Hybrid assistive system-the motor neuroprosthesis. *IEEE Transactions on Biomedical Engineering*, 36(7):729–737, 1989.

[28] J. Rose and J. Gamble. *Human Walking*. LWW medical book collection. Lippincott Williams & Wilkins, 2006.

[29] S. K. Sabut, R. Kumar, and M. Mahadevappa. Design of an insole embedded foot pressure sensor controlled fes system for foot drop in stroke patients. In *Systems in Medicine and Biology (ICSMB), 2010 International Conference on*, pages 237–241. IEEE, 2010.

[30] L. R. Sheffler, P. N. Taylor, D. D. Gunzler, J. H. Buurke, M. J. Ijzerman, and J. Chae. Randomized controlled trial of surface peroneal nerve stimulation for motor relearning in lower limb hemiparesis. *Archives of physical medicine and rehabilitation*, 94:1007–1014, June 2013.

[31] STMicroelectronics . Stm32f427xx/stm32f429xx datasheet - production data. `http://www.st.com/content/ccc/resource/technical/document/datasheet/03/b4/b2/36/4c/72/49/29/DM00071990.pdf/files/DM00071990.pdf/jcr:content/translations/en.DM00071990.pdf`. DocID024030 Rev. 9.

[32] W. Svensson and U. Holmberg. Ankle-foot-orthosis control in inclinations and stairs. In *Robotics, Automation and Mechatronics, 2008 IEEE Conference on*, pages 301–306. IEEE, 2008.

[33] D. Tedaldi, A. Pretto, and E. Menegatti. A robust and easy to implement method for imu calibration without external equipments. In *Robotics and Automation (ICRA), 2014 IEEE International Conference on*, pages 3042–3049. IEEE, 2014.

[34] M. W. Whittle. *Gait analysis: an introduction*. Butterworth-Heinemann, 2014.

[35] D. Winter. *The biomechanics and motor control of human gait*. University of Waterloo Press, 2 edition, 1991.